Dynamic Analysis of a Two Member Manipulator Arm
NAG1-1997
FRS No. 4-42011
Progress Report

Dr. W. Mark McGinley and Dr. Ji Y. Shen
New Co-principal Investigators
Department of Architectural Engineering
North Carolina A & T State University
Greensboro NC 27411

The following report summarizes the activity carried out under the NASA Grant entitled " Dynamic Analysis of a Two Member Manipulator Arm" **NAG1-1997** from March 16, 1996 through March 16, 1997.

This investigation was originally proposed by Dr. Elias Abu-Saba and he was the principal investigator when the grant was awarded. However, Dr. Abu-Saba retired from the North Carolina A & T State University, on August 15, 1995. Since Dr. Abu-Saba has retired, no work has been done on this project. In December, 1995, both Dr. Shen and McGinley expressed an interest in completing this work. After discussions with the technical monitor of the project, Dr. R. Montgomery, application procedures were started to approve replacement of the Principal Investigator on this NASA Grant. The request asked that Dr. W. Mark McGinley and Dr. Y. Shen be made Co-PI's on this project.

Since receiving authorization to work on this project, a computer model has been developed and a number of simulations have been run. The attached DRAFT paper summarizes the model and the result of the simulations. It appears that this method of damping vibrations has great potential.

During this period of the project, a NO-COST Extension was applied for and granted so that the new ending date of the project will be July 31, 1997. This extension was sought to allow Dr. Shen to finish the modifications of the attached paper and present at the Space Studies Institute - Conference of Space Manufacturing, May 8 - 11, 1997.

Draft Technical Paper for the Space Studies Institute - Conference of Space Manufacturing, May 8 - 11, 1997.

End-Effector Vibration Suppression of a Flexible Manipulating System by Using Piezoelectric Actuators

Ji Y. Shen, William M. McGinley and Lonnie Sharpe, Jr.
Dept. of Architectural Engineering, College of Engineering
North Carolina A&T State University, Greensboro, NC 27411

Abstract

Attenuating start-up and stopping vibrations when maneuvering large payloads attached to flexible manipulator systems is a great concern for many space missions. To address this concern, it was proposed that the use of smart materials, and their applications in smart structures, may provide an effective method of control for aerospace structures. In this paper, a modified finite element model has been developed to simulate the performance of piezoelectric ceramic actuators, and was applied to a flexible two-arm manipulator system. Connected to a control voltage, the piezoelectric actuators produce control moments based on the optimal control theory. The computer simulation modeled the end-effector vibration suppression of the NASA manipulator testbed for berthing operations of the Space Shuttle to the Space Station. The results of the simulation show that the bonded piezoelectric actuators can effectively suppress follow-up vibrations of the end-effector, stimulated by some external disturbance.

Introduction

The handling of a large spacecraft using a robotic manipulator is an important technology for future space missions. These operations require precision telerobotic maneuvering of large payloads using the Remote Manipulator System (RMS) of the Space Shuttle. During start-up and stopping, the direction of motion of a large payload is difficult to predict because of start-up transient impulses and the subsequent vibration in the system produced by the flexibility of the manipulator-coupled system. One solution to this vibratory control problem is to conduct the operation slowly, in steps, and minimize the excitation. However, if objectionable vibrations do occur, then extra time is required for them to settle out. This solution will extend the time required for operations, and since the cost of orbit time is extreme high, the cost effectiveness of the mission will be

reduced. In an effort to find more cost effective solutions, NASA continues to develop telerobotic technology that addresses these problems[1,2]. As part of the effort described above, this investigation proposed to develop a methodology for end-effector vibration suppression on a flexible manipulator system by using piezoelectric actuators.

The rapid development of the smart materials and their applications in smart structures shows great potential for the control of aerospace structures. Piezoelectric actuators, as a specific set of these smart materials, appear the most appropriate for this application. In general, two basic approaches, passive damping and active vibration control, have been studied for the control of smart structures[3,4,5]. Structures with bonded/embedded sensors and actuators made of piezoelectric materials are examples of actively controlled structures. In addition, the high stiffness of some piezoelectric materials, typically a ceramic, provides an advantage over viscoelastic materials as a passive damping mechanism. The material properties of the piezoelectric ceramic also has the advantage of being relatively stable with temperature over their operating range.

A linear elastic finite element model for piezo-layer bonded beams, based on general finite element approach, had been developed in the authors' previous work. The previous investigation applied a modified finite element model to the optimal controller design for vibration suppression of a cantilevered composite beam[6]. This approach is extended by the investigation described in this paper, and includes the development of a joint element for the end-effector vibration suppression of a flexible two-arm manipulating system.

The system studied in this investigation is the NASA manipulator testbed for the research of berthing operations of the space shuttle to the space station, which consists of two flexible links and three revolute joints. This testbed was assumed to be constrained in the horizontal plane for the modeling and analysis. Figure 1 shows a schematic representation of the testbed. Each of the two links shown can be modeled as individual frame elements, some with bonded piezoelectric actuators. In response to a control voltage, the piezoelectric actuators can produce control moments and be used to dampen vibrations of the manipulator arm.

The following sections describe the model development and summarize the computer simulation results. This simulation was conducted on the modeled manipulator system, and assumes that an external disturbance causes an initial deflection in one of the arms. This initial deflection stimulates a vibration of the manipulator system and the

bonded piezoelectric actuators are used to suppress the follow-up vibration of the end-effector, using control signals based on the optimum control theory.

Modified Finite Element Model for the Piezo-Layer Bonded Beam

The general finite element model for deflection analysis of beam-like structures can be characterized by:

$$[M]\{\ddot{y}\}+[K]\{y\}=\{F\} \tag{1}$$

For each beam element, the nodal displacement vector consists of the axial and lateral displacements and slopes at the two nodal points, that is, $\{y\}_i=\{u_i,v_i,\theta_i,u_{i+1},v_{i+1},\theta_{i+1}\}^T$, and the nodal force vector consists of axial forces, shears and bending moments at the same nodal points, that is, $\{f\}_i=\{V_i,Q_i,M_i,V_{i+1},Q_{i+1},M_{i+1}\}^T$. The stiffness matrix $[k]_i$ and the consistent mass matrix $[m]_i$ of the *ith* beam element take the forms of [7]

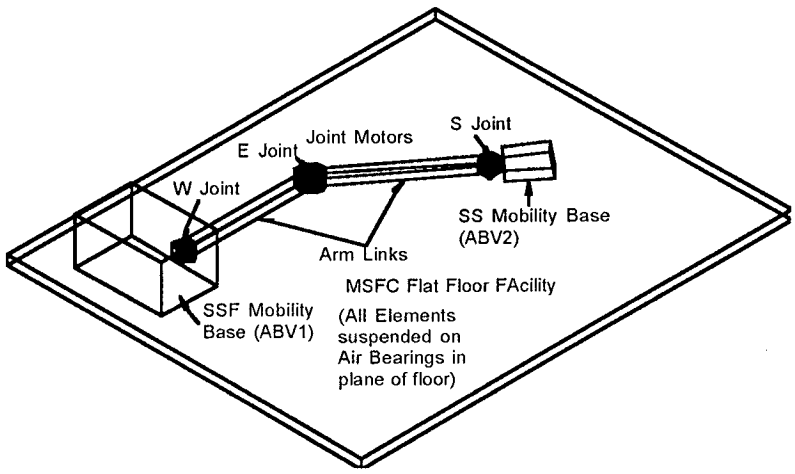

Fig. 1 Schematic Diagram of the NASA Manipulator Testbed

$$[k]_i = \begin{bmatrix} \frac{E_iA_i}{l_i} & 0 & 0 & -\frac{E_iA_i}{l_i} & 0 & 0 \\ 0 & \frac{12E_iI_i}{l_i^3} & \frac{6E_iI_i}{l_i^2} & 0 & -\frac{12E_iI_i}{l_i^3} & \frac{6E_iI_i}{l_i^2} \\ 0 & \frac{6E_iI_i}{l_i^2} & \frac{4E_iI_i}{l_i} & 0 & -\frac{6E_iI_i}{l_i^2} & \frac{2E_iI_i}{l_i} \\ -\frac{E_iA_i}{l_i} & 0 & 0 & \frac{E_iA_i}{l_i} & 0 & 0 \\ 0 & -\frac{12E_iI_i}{l_i^3} & -\frac{6E_iI_i}{l_i^2} & 0 & \frac{12E_iI_i}{l_i^3} & -\frac{6E_iI_i}{l_i^2} \\ 0 & \frac{6E_iI_i}{l_i^2} & \frac{2E_iI_i}{l_i} & 0 & -\frac{6E_iI_i}{l_i^2} & \frac{4E_iI_i}{l_i} \end{bmatrix}$$

$$[m]_i = m_i \begin{bmatrix} \frac{1}{3} & 0 & 0 & \frac{1}{6} & 0 & 0 \\ 0 & \frac{13}{35} & \frac{11l_i}{210} & 0 & \frac{9}{70} & -\frac{13l_i}{420} \\ 0 & \frac{11l_i}{210} & \frac{l_i^2}{105} & 0 & \frac{13l_i}{420} & -\frac{l_i^2}{140} \\ \frac{1}{6} & 0 & 0 & \frac{1}{3} & 0 & 0 \\ 0 & \frac{9}{70} & \frac{13l_i}{420} & 0 & \frac{13}{35} & -\frac{11l_i}{210} \\ 0 & -\frac{13l_i}{420} & -\frac{l_i^2}{140} & 0 & -\frac{11l_i}{210} & \frac{l_i^2}{105} \end{bmatrix}$$

where, l_i is the length of the ith beam element, $m_i = \rho A_i l_i$ its mass, E_iI_i its flexural rigidity.

If a piezo-layer is bonded to one surface of a beam element, the neutral axis of the composite section will change its location (D = depth of neutral axis, Figure 2), and this location can be determined based upon the force balance in the longitudinal direction of the element[6],

$$D = \frac{1}{2[E_p h_p + E_b h_b]}\left[E_p h_p^2 + E_b h_b^2 + 2E_p h_p h_b\right] \qquad (2)$$

Figure 2 shows a schematic drawing of a piezo-layer bonded beam element, where, l_i is the length of the ith element, b is the width, h_p and h_b are the thickness of the piezo-actuator and the beam respectively, M_p is the bending moment applied to the actuator and M_b is the bending moment applied to the beam. The equivalent flexural rigidity E_iI_i for the ith composite beam can be computed based upon $(E_iI_i)_p$ and $(E_iI_i)_b$ through the expression

$$E_i I_i = E_{i_p} I_{i_p} + E_{i_b} I_{i_b} \tag{3}$$

(Note that these I values are computed about the neutral axis of the composite section.)

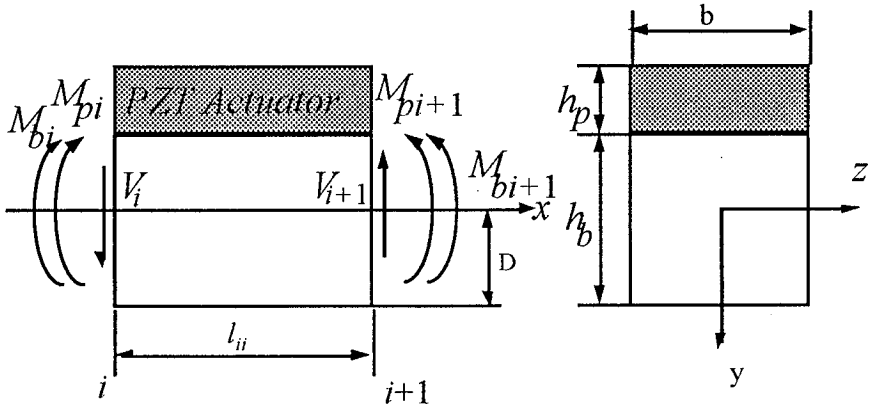

Fig. 2 The *ith* Element of a Composite Beam

If a voltage ***e*** is applied to the piezoelectric actuator, an average normal strain, $\varepsilon_p = [d/h_p]e$, is introduced in the layer, where d is the electric charge constant of the piezoelectric material. This strain results in a normal stress $\sigma_p = E_p[d/h_p]e$, which produces a bending moment as given by, $M_p = \int_{D-h_b}^{D-(h_b+h_p)} \sigma_p (by) dy$. Substitution of the expressions for σ_p and D into the expression for M_p , we find that

$$M_p = c_p e \tag{4}$$

where, $c_p = \dfrac{dbE_p E_b h_b [h_p + h_b]}{2[E_p h_p + E_b h_b]}$ is the control-moment coefficient.

In summary, it is clear from the above development that a conventional finite element model can be formulated for the piezo-layer bonded beam-like structure if following modifications are made: (1) the location of the neutral axis of the element is specified by D, (Eq. 2); (2) the equivalent flexural rigidity $E_i I_i$ of the element accounts for the composite material behavior, (Eq. 3); (3) the *ith* element force vector $\{f\}_i$ includes the piezo-layer bending moment M_p , that is,
$\{f\}_i = [V_i, Q_i, M_{b_i} + M_{p_i}, V_{i+1}, Q_{i+1}, M_{b_{i+1}} + M_{p_{i+1}}]^T$.

Stiffness Matrix of a Revolute Joint

The function of a revolute joint is to connect two links of a kinematic assemblage. The connected links can have relative rotational motion, but the two nodes (say, I and J) on each of the connected elements, respectively, remain coincident with each other (the compatibility condition). For a planar manipulating system, each node has three degrees of freedom, that is, the translational motions u and v, and rotational motion θ. Since a joint consists of two nodes I and J, even though they are coincident, a joint will still have six degrees of freedom. Assuming that the translational stiffnesses are represented by translational spring constants k_x and k_y, and the rotational stiffness by rotational spring constant k_θ, the compatibility condition and moment equilibrium will produce the following six equations at each joint: (in matrix form),

$$\begin{bmatrix} k_x & 0 & 0 & -k_x & 0 & 0 \\ 0 & k_y & 0 & 0 & -k_y & 0 \\ 0 & 0 & k_\theta & 0 & 0 & -k_\theta \\ -k_x & 0 & 0 & k_x & 0 & 0 \\ 0 & -k_y & 0 & 0 & k_y & 0 \\ 0 & 0 & -k_\theta & 0 & 0 & k_\theta \end{bmatrix} \begin{Bmatrix} u_i \\ v_i \\ \theta_i \\ u_j \\ v_j \\ \theta_j \end{Bmatrix} = \begin{Bmatrix} 0 \\ 0 \\ \tau \\ 0 \\ 0 \\ -\tau \end{Bmatrix} \tag{5}$$

where, the coefficient matrix, designated as $[k]_R$, is the stiffness matrix of a *Joint R*, and τ is the joint moment. Note that $[k]_R$ is singular for an individually joint, that is, $Det[k]_R=0$, but it will not bring singularity into the global system, since the global system requires superposition to be applied at each joint. The inertia of the joint was assumed to be negligible and therefore neglected.

Optimal Controller Design for End-Effector Vibration Suppression

Ignoring any inherent passive damping effects, the system equation can be written in the state-space form, that is,

$$\{\dot{X}\} = [A]\{X\} + [B]\{u\} \tag{6}$$

where, the state vector is defined as $\{X\} = \{x_1, x_2\}^T = \{y, \dot{y}\}^T$, the system matrix, $[A] = \begin{bmatrix} 0 & I \\ -M^{-1}K & 0 \end{bmatrix}$, the control influence matrix, $[B] = \begin{bmatrix} I & 0 \\ 0 & M^{-1} \end{bmatrix}$, and the control (force) vector, $\{u\} = \{0, F\}^T$.

According to the optimal control theory[8], the linear quadratic performance index, J, can be formulated as

$$J = \frac{1}{2}\int_0^\infty \left(X^T Q X + u^T R u\right) dt \tag{7}$$

The optimal controller solution for this linear quadratic regulator problem is $u=-R^{-1}PX$, where matrix $[P]$ can be obtained from the steady-state matrix Riccati equation, $A^T P+PA-PBR^{-1}B^T P=-Q$.

The solution to the state-space equation, (Eq. 6), can be obtained from a recursive formula provided that the initial conditions $\{X\}_0$ are known[9], that is,

$$\{X\}_{i+1} = e^{A\Delta t}\{X\}_i + [A]^{-1}\left(e^{A\Delta t} - I\right)[B]\frac{\{u\}_i + \{u\}_{i+1}}{2} \tag{8}$$

where, the matrix exponential $e^{A\Delta t}$ is defined as $e^{A\Delta t} = I + A(\Delta t) + \frac{A^2(\Delta t)^2}{2!} + \frac{A^3(\Delta t)^3}{3!} + \cdots\cdots$, and consequently, $A^{-1}(e^{A\Delta t} - I) = I(\Delta t) + \frac{A(\Delta t)^2}{2!} + \frac{A^2(\Delta t)^3}{3!} + \cdots\cdots$.

However, if the optimal control solution has been found, then the state-space equation (Eq. 6) can be simplified as

$$\{\dot{X}\} = [\overline{A}]\{X\} \tag{9}$$

where the new system matrix with implementation of optimal control is defined as $[\overline{A}] = [A] - [B][R]^{-1}[B]^T[P]$. The same method described above for the full state-space equation, (Eq. 6), can be used to solve this simplified version (Eq. 7). If the stiffness and mass matrices incorporate the models of the composite elements and joints described in the previous sections, then the resulting solution of Eq. 9, will model the behavior of the two arm system over time.

Computer Simulation

The system used to test the model and analysis techniques described previously was the NASA manipulator Testbed for the research of the Space Shuttle to the Space Station berthing operations. This research testbed is designed to model the berthing process, but is constrained to

motions in the horizontal plane[1]. Figure 1 illustrates the principal components of the facility. The Space Station Freedom (SSF) Mobility Base is an existing Marshall Space Flight Center (MSFC) Vehicle that has a mass of *2156.4 kg*, and is referred to, herein, as Air Bearing Vehicle 1 (ABV1). It represents the Space Station in the berthing operation, and is considered a payload on the end-effector. This vehicle is levitated on the MSFC flat floor facility using low flow-rate bearings. The other vehicle, the Space Shuttle (SS) Mobility Base, designated as Air Bearing Vehicle 2 (ABV2), is attached to the wall of the flat floor facility through the shoulder joint, and can be connected to the SSF Mobility Base with a flexible two-arm manipulator system. Each of these arms are made of a *2.74 m* long aluminum I-beam with a mass of *37.089 kg*, the flanges of which are *0.076 m* by *0.0032 m* and the web is *0.1 m* by *0.0032 m*. There are three revolute joints: shoulder joint S, elbow joint E, and wrist joint W.

Since the dimension of the end-effector with the payload can not be, in general, comparable with dimensions of the two arms, the end-effector will be modeled as a rigid body with a mass point at the wrist joint. The elbow joint (E Joint) and wrist joint (W Joint) are supported by air bearings. If it is assumed that the shoulder joint (S Joint) and elbow joint are independently driven by individual actuators, the control moments τ_s and τ_e act on the revolute joints S and E, respectively. The joint compliances are characterized by three spring constants: k_x in x-direction, k_y in y-direction, and k_θ for rotation. The corresponding input joint torques are transmitted through the arm linkage to the end-effector, where the resultant force and moment act upon the Space Station Freedom Mobility Base (*ABV1*). For the simulation, each link was divided into five frame elements. The numbering system for finite elements and nodal points are as shown in Figure 3.

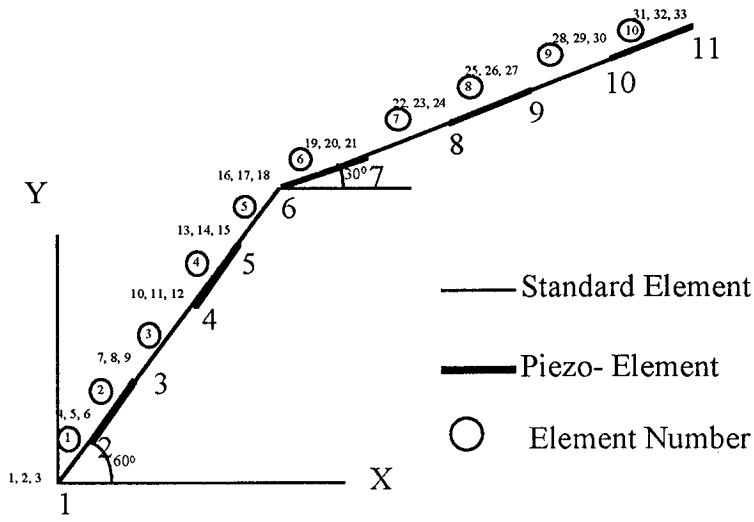

Fig. 3 A Finite Element Model of A Flexible Two-Arm Manipulator System with Piezoelectric Actuators Bonded on Some of the Elements

The initial system configuration for computer simulation was assumed as follows. The up-arm (elements 6 through 10) formed a 60^0 angle with the global X-axis, and the forearm (elements 1 through 5) formed a 30^0 angle with the horizontal. Because the two arms are not in the same orientation, it is necessary to account for the alignment of the two arms. The coordinate transformation matrix between the local element coordinate system z-y and the global coordinate system Z-Y can be expressed as

$$[L] = \begin{bmatrix} l & m & 0 & 0 & 0 & 0 \\ -m & l & 0 & 0 & 0 & 0 \\ 0 & 0 & 1 & 0 & 0 & 0 \\ 0 & 0 & 0 & l & m & 0 \\ 0 & 0 & 0 & -m & l & 0 \\ 0 & 0 & 0 & 0 & 0 & 1 \end{bmatrix}$$

where, the direction cosines are $l=cos(x,X)$, and $m=cos(x,Y)$, respectively. The element stiffness matrix in global coordinate system is then $[k]_i = [L]^T[k']_i[L]$, where $[k']_i$ is the element stiffness matrix in local coordinate system. The same transformation was also applied to the element mass matrix. In addition, the element nodal load vector in global coordinate

system can be obtained by $\{f\}_i = [L]^T \{f'\}_i$, where $\{f'\}_i$ is the element nodal load vector in local coordinate system.

For aluminum, the elastic modules was taken as, $E_b = 7.6 \times 10^8 N/m^2$, and density as $\rho = 2840 kg/m^3$. The second moment of area for the given *I*-beam cross-section $I_b = 0.1562 \times 10^{-5} m^4$. For convenience, an equivalent rectangular cross section with height $h=0.0627$ *m* and width $b=0.076$ *m* is used in simulation, which provides the same value of the second moment of area. It was also assumed that the piezoelectric ceramic actuators, with thickness $h_p=0.003$ *m*, were bonded on one side of the frame elements *2, 4, 6, 8,* and *10*. The piezoelectric layers were assumed to have the following properties: elastic modules $E_p = 6.3 \times 10^8 N/m^2$, second moment of area $I_p = 0.224 \times 10^{-6} m^4$, the electric charge constant $d = 5.3 \times 10^{-10} m/v$.

During the computer simulations both weighting function matrices, *[Q]* and *[S]* were set equal to the identity matrix. This assumes that each action will have equal weight on control. Further study of the actual values of these matrices may improve the effectiveness of this control strategy and should be the subject of further study.

It can be assumed that an external disturbance causes an initial deflection of the forearm. In the simulations, the forearm nodes 7, 9, 11 were assumed to have an initial *0.01 m* deformation parallel to the *X*-axis and *0.1 m* initial deformation parallel to the *Y*-axis. Nodes *8* and *10* were assumed to have the same deformations, but in opposite directions. These initial deformations would then result in a vibration of the manipulator system, when released. The computer simulation predicted the response of the system after released and under the action of optimal control moments provided by the piezoelectric actuators. The computational results show that bonded piezoelectric actuators can effectively suppress the follow-up vibration of the end-effector as shown in Figures 4 and 5, where Figure 4 indicates the decayed time history of node 11 in *X*-direction, and Figure 5 indicates the decayed time history of node 11 in *Y*-direction.

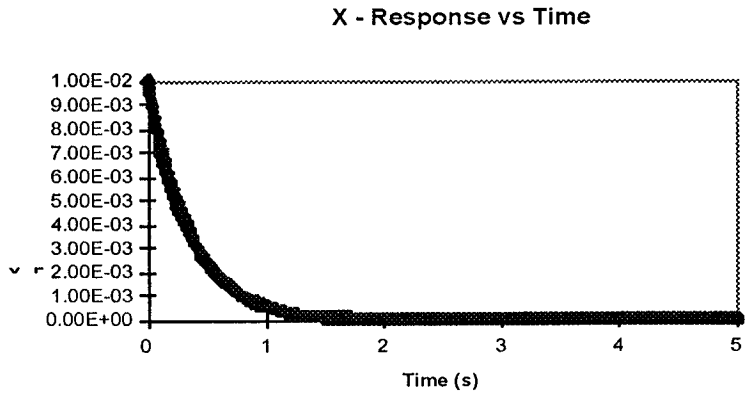

Fig. 4 The Decayed Response Time History of the End-Effector in the X-Direction

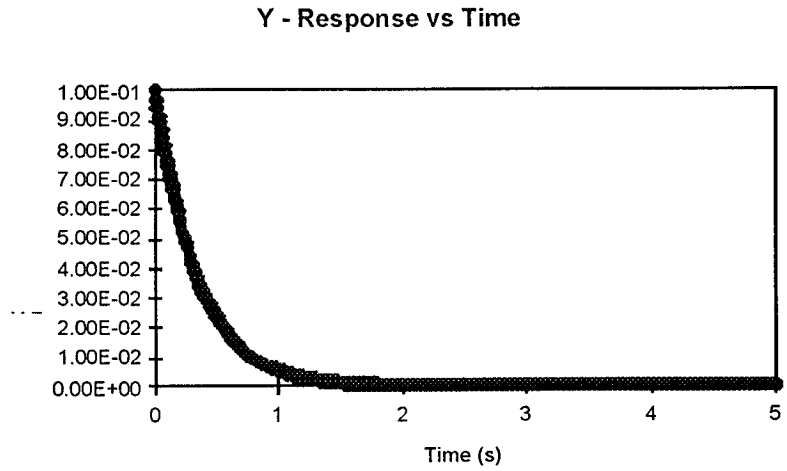

Fig. 5 The Decayed Response Time History of the End-Effector in the Y-Direction

Concluding Remarks

A modified linear elastic finite element model, based on the general finite element method, has been developed to include the effects of piezoelectric ceramic actuators. This model has been applied to the end-effector vibration suppression of a flexible two-arm manipulator system. The control methodology uses an optimized technique that appears to effectively attenuate system vibrations and thus may be an effective means to control start-up and stopping vibrations present when maneuvering large payloads on space missions.

Acknowledgments

This research was funded by NASA Langley Research Center under Contract Number NAG1-997. Many thanks to Dr. Raymond C. Montgomery at NASA Langley Research Center for his guidance and valuable suggestion throughout the course of this study. The authors are deeply indebted to Dr. Elias G. Abu-Saba, who initiated a proposal for this research topic.

References

1. Montgomery, R.C., Tobbe, P.A., et al, "Simulation and Testing of a Robotic Manipulator Testbed", the 10th VPI&SU Symposium on Structural Dynamics & Control, Blacksburg, VA. May 8-10, 1995.
2. Montgomery, R.C., Tobbe, P.A., et al, "A Testbed for Research on Manipulator-Coupled Active Spacecraft", AIAA Guidance, Navigation, and Control Conference, Monterey, CA. August 1993.
3. Rogers, C.A., "Active Vibration and Structural Acoustic Control of Shape Memory Alloy Hybrid Composites: Experimental Results," Journal of Acoustic Society, Am.90(1), 1990, pp2803-2811.
4. Baz, A. and Poh, S., "Performance of an Active Control System with Piezoelectric Actuators." J. of Sound and Vibration, Vol.126, No.2, pp327-343.
5. Crawley, E.F. and de Luis, J., "Use of Piezoelectric Actuators as Elements of Intelligent Structures." AIAA Journal, Vol.25, No.10, pp1373-1385.
6. Shen, J.Y., Lonnie Sharpe, Jr. and Lu, M.F., "Optimal Control of Beam Vibration Suppression", Proceedings of the 10th Engineering Mechanics Conference, ASCE, Boulder, CO. May 21-24,1995, pp.1070-1073.
7. Chandrapatla, T.A. and Belegundu, A.D., Introduction to Finite Elements in Engineering", Prentice Hall, 1991.
8. Bryson, A.E. and Ho, Y.C., "Applied Optimal Control: Optimization, Estimation and Control", Hemisphere Publishing Corporation, 1975.
9. Shen, J.Y. and Lonnie Sharpe, Jr., "Estimation of Physical Damping Parameter by Using Maximum Likelihood Estimator", Proceedings of the 8th Southeastern Conference on Theoretical and Applied Mechanics, Tuscaloosa, Alabama, April 14-16, 1996.